

**Supplementary data**

**GRIM-19 inhibits v-Src-induced cell motility by interfering with  
cytoskeletal restructuring**

**Peng Sun\*<sup>\$</sup>, Shreeram C. Nallar\*, Sudhakar Kalakonda, Daniel J.**

**Lindner<sup>¶</sup>, Stuart S. Martin<sup>&</sup> and Dhananjaya V. Kalvakolanu<sup>\$\$&</sup>**

\*Department of Microbiology & Immunology, <sup>&</sup>Greenebaum Cancer Center, University of  
Maryland School of Medicine, Baltimore, MD 21021. <sup>\$</sup>Molecular and Cellular Cancer  
Biology graduate track, The Graduate Program in Life Sciences, University of Maryland  
Baltimore. <sup>¶</sup>Taussig Cancer Center and Department of Cancer Biology , The Cleveland Clinic  
Lerner Research Institute, Cleveland, OH 44195

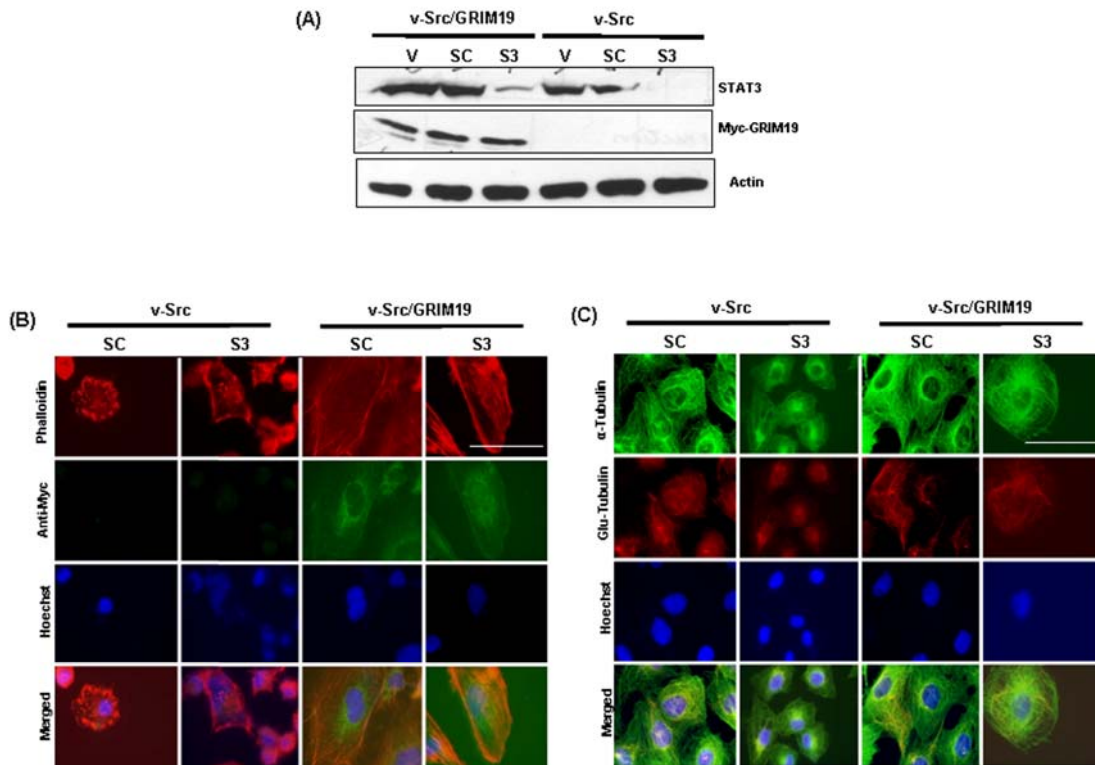


**Fig. S1: Effect of STAT3-specific shRNA on v-Src induced cytoskeletal reorganization and inhibitory role of GRIM-19 on v-Src.** (A) Western blot analysis of the STAT3 shRNA-mediated knockdown of STAT3. (B) Effect of GRIM-19 on v-Src-induced podosome formation and exogenous GRIM-19. Magnification: 100X (C) Detection of tubulin and detyrosinated tubulin with immunofluorescent staining. Magnification: 100X V: *pLK0.1* vector; SC: scramble shRNA; S3: STAT3 shRNA. Scale bar, 50 $\mu$ m.

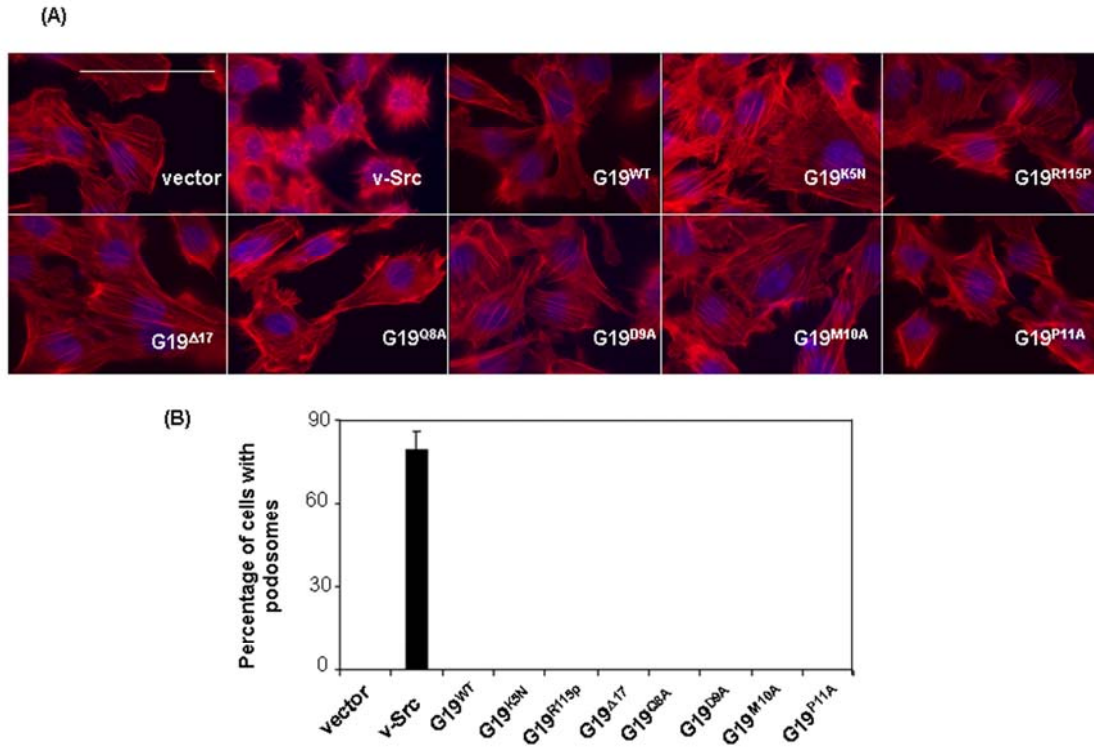


**Fig. S2: Expression of GRIM-19 mutants alone did not induce podosome formation in 3Y1 cells.** (A) Immunofluorescent staining of v-Src transformed 3Y1 cells and 3Y1 cells expressing empty-vector, wildtype GRIM-19 and GRIM-19 mutants with phalloidin for actin and Hoechst for DNA. Magnification: 100X. Scale bar, 50 $\mu$ m. (B) v-Src transformed 3Y1 cells and 3Y1 cells expressing empty vector, wildtype GRIM-19 and GRIM-19 mutants were counted according to the percentage of cells containing podosome.

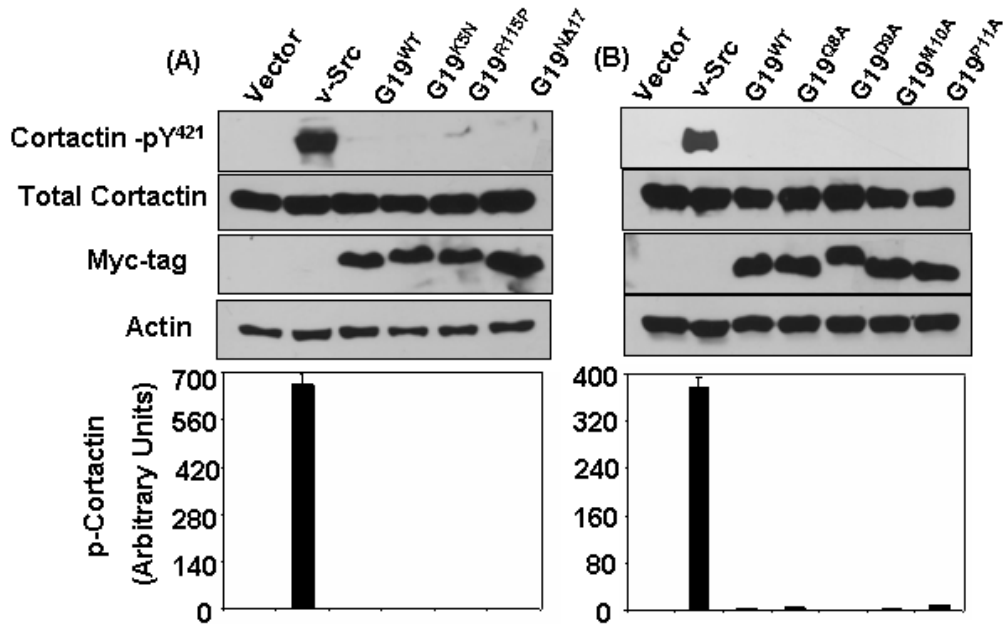


**Fig. S3: Expression of GRIM-19 mutants alone did not cause cortactin phosphorylation in 3Y1 cells. (A&B)** Western blot analysis of v-Src transformed 3Y1 cells expressing empty vector wildtype GRIM-19 and GRIM-19 mutants. The graph below each Western blot showed the comparison of the relative optical density (Arbitrary unit) of cortactin phosphorylation status. The optical density of cortactin phosphorylation was normalized against the expression levels of endogenous cortactin and exogenous wildtype GRIM-19 and GRIM-19 mutants. Mean band intensity  $\pm$ SE of 4 independent samples is shown in each case.

**Table S1: Primer sequences used for generating GRIM-19 constructs**

<b>ID</b>	<b>Sequence (5'-3')</b>
WT	GCG <b>GAATTC</b> GCCACCATGGCGGCGTCAAAGGTG
K5N	GCG <b>GAATTC</b> GCCACCATGGCGGCGTCAaacGTGAAG
Q8A	GCG <b>GAATTC</b> GCCACCATGGCGGCGTCAAAGGTGAAGgcgGACATG
D9A	GCG <b>GAATTC</b> GCCACCATGGCGGCGTCAAAGGTGAAGCAGgcgATGCC
M10A	GCG <b>GAATTC</b> GCCACCATGGCGGCGTCAAAGGTGAAGCAGGACgcgCCTCC
P11A	GCG <b>GAATTC</b> GCCACCATGGCGGCGTCAAAGGTGAAGCAGGACATGgcgCCGCC
$\Delta$ 1-17	GCG <b>GAATTC</b> GCCACCATGCCCATCGACTACAAGCGGAAC
R115Pf	TCCACACAACCcccTGGGTGC
R115Pr	ACCCAgggGGTTGTGTGGAAC
Rev	CAG <b>GGATCCC</b> GTGTACCACATGAAGCCG

GRIM-19 R115P mutant amplicon for cloning was obtained by pooling two half-reactions that employed R115P-specific and compatible (WT/Rev) primers in PCR. In the primer sequence, restriction enzyme sites and mutant codons are represented in bold and lower-case alphabets, respectively.